Analysis of Chaos-Based Code Tracking Using Chaotic Correlation Statistics

Ramin Vali, Stevan M. Berber, and Sing Kiong Nguang

***Abstract*—A new statistical method for examining correlation of chaos-based systems is presented and the proposed method is applied to the analysis of a chaos-based noncoherent tracking loop. The motivation behind this approach is the lack of accuracy in the treatment of chaos-based code tracking when conventional correlation analysis is used. The proposed method has it roots in the chaotic correlation statistics (CCS) of the chaotic spreading code. CCS can be used for chaotic as well as any other nonbinary spreading code. The accuracy of the proposed model is shown to be very high by means of comparison with simulation and implementation results. The distributions of two critical points on S-curve have been derived and shown to closely match the simulation results as well as hardware implementation results. This paper highlights the need for a statistical approach for accurate treatment of nonbinary spreading codes specifically chaos-based spreading codes.**

***Index Terms*—Chaos-based code tracking, chaos-based communications, chaos-based correlation, chaotic statistical analysis, digital signal processing, noncoherent tracking.**

I. Introduction

MUCH RESEARCH has been aimed at applying chaos theory in telecommunications in general and spread spectrum communications in particular. There are three main reasons for such interest in chaos-based communications. The first reason is related to signal masking which is achievable on a physical level for spread spectrum communications [1], [2]. The second reason is related to the inherent wide bandwidth that chaotic spreading codes occupy making them very suitable for wide-band communications [3], [4]. Finally and perhaps the most important reason is the orthogonality of chaotic spreading codes. That is, chaotic spreading codes generated from the same map with different initial conditions are orthogonal [5]. These three features of chaotic spreading codes make them very competitive candidates for spreading code of choice in spread spectrum communications. As a result, much research has been directed at various chaos-based communication schemes [4]–[9].

In a direct sequence spread spectrum (DS-SS) context, the spreading code generators in transmitter and receiver have to *acquire* and *maintain* synchronization with each other [10]–[14]. Without accurate synchronization, despreading of the signals cannot be performed. Acquiring synchronization is preformed by the acquisition stage which estimates the time delay between the transmitter and receiver to within one chip duration. The acquisition stage of systems using chaotic spreading codes has been covered extensively in the literature and is not the primary focus of this paper.

The maintenance of synchronization between the transmitter and receiver is achieved through code tracking which has the role of estimating the transmitter-receiver time delay to less than a chip duration. The tracking stage tracks the code timing in the presence of timing jitter which is caused by clock drift and other imperfections in the transmitter, receiver and wireless channel. Many tracking architectures have been proposed but the most popular one is the delayed lock loop (DLL) which was first proposed in [13] and later on expanded in [14].

The DLL relies on two correlators, one advanced and one delayed in time by a certain fraction of chip time. The output of the DLL is the difference of the two correlations. This difference, when plotted against time, is known as an error curve or an S-curve which is used to compensate for the advances and delays resulting from the timing jitter. It is imperative for the S-curve to have a high degree of accuracy, otherwise the tracking loop will not compensate for the jitters properly.

There have been several examinations of chaos-based code tracking loops [15]–[21] that utilize correlation of chaos-based sequences. The common point in all these investigations is the assumption that the correlation function of the chaotic sequence remains constant for different chaotic spreading codes generated from the same chaotic map. However, this assumption is based on the treatment of conventional spreading codes such as PN codes, Walsh functions, etc., that are binary. Chaotic spreading codes on the other hand, are nonbinary and can take any value between two set bounds. Therefore, for different initial conditions the chaotic correlation function changes. This means that applying the conventional theoretical models to chaotic spreading codes can only give an approximation to the true behavior of the chaos-based correlation function.

In order to properly examine the behavior and performance of chaotic spreading codes in code tracking, the true statistics of the correlation functions involved have to be taken into account. This is achieved by statistically describing the chaos-based correlation function using chaotic correlation statistics (CCS). To the best of the authors' knowledge, there is no treatment of chaos-based tracking that involves the usage of CCS. The aim and contribution of this paper is to examine the chaos-based noncoherent tracking loop using CCS for the first time. The accuracy of CCS is shown to be very high when compared to the simulation results.

Manuscript received February 17, 2011; revised June 22, 2011; accepted August 19, 2011. This paper was recommended by Associate Editor G. Setti.

The authors are with the Department of Electrical and Computer Engineering, The University of Auckland New Zealand, Auckland 1142, New Zealand (e-mail: r.vali@ieee.org; s.berber@auckland.ac.nz; sk.nguang@auckland.ac.nz).

Color versions of one or more of the figures in this paper are available online at http://ieeexplore.ieee.org.

Digital Object Identifier 10.1109/TCSI.2011.2169885

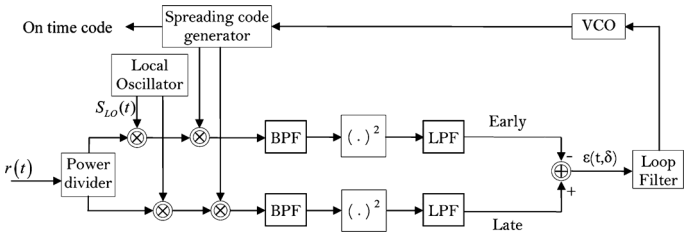

Fig. 1. Noncoherent tracking loop block diagram [16].

The rest of this paper is structured as follows. Section II gives a very brief introduction to the conventional treatment of chaos-based noncoherent tracking loop. Section III details the statistical treatment of the chaotic correlation function which forms the basis of the new approach. Section IV presents the application of the newly developed statistical approach to the chaos-based noncoherent tracking problem. Section V shows the comparison between the analytical and simulation results. Section VI presents the conclusions.

II. Theoretical Model of a Chaos-Based Non-Coherent Tracking Loop

This section presents a very brief introduction to the chaos-based noncoherent tracking loop. Detailed explanations and derivations for chaos-based tracking can be found in [16]–[18]. As can be seen from Fig. 1 the noncoherent tracking loop presented here employs two correlators; one advanced in time and one delayed in time. These two give the correlations of the transmitter pilot signal with the locally generated receiver pilot signal. Since code tracking starts after code acquisition, it is assumed that the relative delay between the transmitter and receiver codes is known to within one chip duration (T_c). The output of the two correlators are squared and subtracted from each other. The result of this subtraction is the most important parameter in the loop operation $\epsilon(t,\delta)$. This expression is derived in [16] for chaos-based tracking and is repeated here as (1) at the bottom of the page only for the sake of convenience.

In (1), K_1 and A are filter gain and pilot amplitude respectively, t represents time (discrete in this case), δ is the normalized time difference between the incoming time offset (T_d) and the estimated time offset ($\hat{T}_d$), that is $\delta = T_d - \hat{T}_d/T_c$, Δ is the time separation between the advanced and delayed correlators in chip duration and $R[\cdot]$ is the conventional correlation function. As can be seen from (1), the first line is the desired error expression, which when plotted for different δ gives the S-curve. The rest of the expressions are low pass filtered $\mathrm{signal} \times \mathrm{noise}$ and $\mathrm{noise} \times \mathrm{noise}$ terms; ϕ is the carrier phase and all the terms in the fourth line of the expression are the in-phase and quadrature noise terms from the two branches. This $\epsilon(t,\delta)$ will go through the tracking loop filter which ideally has a bandwidth suitably adjusted to reject all the noise and phase modulated sinusoidal terms. As a result, the input to the voltage controlled oscillator (VCO) is $(1/2)K_1A^2D_\Delta(\delta)$ where $D_\Delta(\delta)$ is the difference between the squared correlation functions shown in the first line of (1) [10], [11], [13], [16]. $D_\Delta(\delta)$ will be filtered using the loop filter where the dc term will be extracted and used as the input to the VCO. In this paper, the loop filter is assumed to be an averaging integrator which has already been explained in [16], [17]. The code generation can be sped up or slowed down to match the incoming timing jitter based on the input value to the VC.

III. Statistical Modeling of Chaotic Correlation Function

As mentioned in the introduction, different initial conditions of the discrete chaotic maps lead to different correlation functions. Therefore, the notion of the correlation function, $R(\tau)$, cannot be realized by a single vector of values. To accurately model the chaos-based tracking loop, it is essential to model the correlation function accurately.

There are many different chaotic sequences in existence and the reader can refer to [22], [23] for good surveys on these signals, more over the synchronization performance of chaotic signals can be found in [24]–[27]. However, the logistic map (a subset of the Chebychev chaotic map) is used for this analysis. This is because most of the chaos-based tracking analysis published in [16]–[18] uses the logistic map and using this map all owes for clear definition of the limitations of the previous analyses and the accuracy of the current analysis.

Chebychev maps are iterative and, in case of the logistic map, the generating equation is $x_{k+1} = 2x_k^2 - 1$[28]. Given that the initial condition for the chaotic map can be any number within $(-1, 1)$ except -0.5, 0.5, and 0, taking all the possible initial conditions into account can only be achieved by assuming the chaotic value to be a random variable, with a certain probability density function (PDF). The Chebychev maps have invariant probability density therefore, the results can be easily extended to any other subset of the Chebychev map [28].

$$
\begin{aligned}
\epsilon(t,\delta) = {} & \frac{1}{2}K_1A^2\left\{R^2\left[\left(\delta-\frac{\Delta}{2}\right)T_c\right]-R^2\left[\left(\delta+\frac{\Delta}{2}\right)T_c\right]\right\} \\
& + \sqrt{2K_1}A\left\{R\left[\left(\delta-\frac{\Delta}{2}\right)T_c\right]n_{2I}(t)-R\left[\left(\delta+\frac{\Delta}{2}\right)T_c\right]n_{1I}(t)\right\}\times\cos(\phi-\phi'+\gamma_d(t-T_d)) \\
& + \sqrt{2K_1}A\left\{R\left[\left(\delta-\frac{\Delta}{2}\right)T_c\right]n_{2Q}(t)-R\left[\left(\delta+\frac{\Delta}{2}\right)T_c\right]n_{1Q}(t)\right\}\times\sin(\phi-\phi'+\gamma_d(t-T_d)) \\
& + \{n_{2I}(t)\}^2+\{n_{2Q}(t)\}^2-\{n_{1I}(t)\}^2-\{n_{1Q}(t)\}^2. \qquad (1)
\end{aligned}
$$

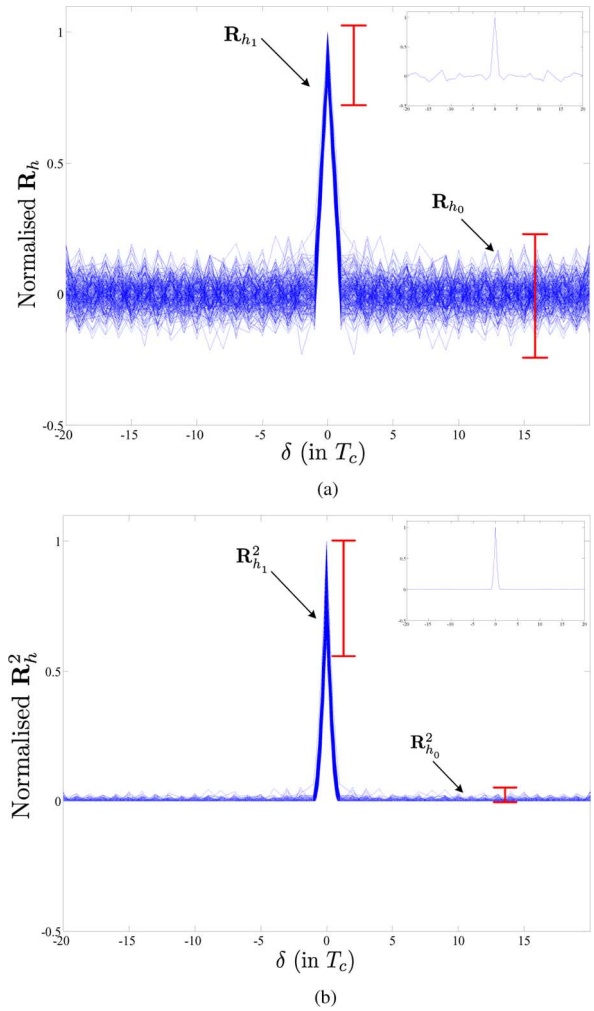

Fig. 2. Normalized correlation function (a) and square of the correlation function (b) for different initial conditions of the logistic map. The assumption used in [9], [15], [18], [29] are shown in the top right of both figures for comparison. (a) Normalized correlation function. (b) Output of the square-law device for one branch.

The PDF of the logistic map is [28]

$$P_x(x) = \begin{cases} \frac{1}{\pi(\sqrt{1-x^2})} & -1 < x < 1 \\ 0 & \text{otherwise.} \end{cases} \tag{2}$$

The mean and variance values can be readily calculated as 0 and $1/2$ respectively. Fig. 2(a) and (b) show the correlation function and square of the correlation function for different initial conditions of the logistic map respectively. Unlike the previous treatments of chaos-based correlation, the correlation function has a distribution and the correlation peak has a different distribution compared to the rest of the correlation function.

Given the statistical properties above, the statistical correlation function of the chaotic map can be written in discrete form as

$$\mathbf{R}_h[\delta] = \sum_{i=1}^{L} (x_{i-\tau} x_{i-\delta}), \tag{3}$$

where $\mathbf{R}_h[\cdot]$ denotes the statistical correlation function which is acquired over h trials, δ is the normalized time delay previously introduced, L is the correlation length, $x_{i-\tau}$ is the transmitter pilot sequence which is being tracked and $x_{i-\delta}$ is the receiver, locally generated, pilot sequence. The difference between $R[\cdot]$ given in (1) and $\mathbf{R}_h[\cdot]$ given above is that $R[\cdot]$ is the conventional correlation function used for binary spreading codes and therefore has the same value if the same correlation length is used, whereas $\mathbf{R}_h[\cdot]$ is a random vector with different distributions along its length.

It is clear from (3) that there are two types of $\mathbf{R}_h[\cdot]$ values. The first type is generated when $x_{i-\tau}$ and $x_{i-\delta}$ are not aligned in time, i.e., $\delta \neq \tau$. Given the orthogonality of chaotic sequences, the resulting value for $\mathbf{R}_h[\cdot]$ has to be close to zero. The second type is generated when $x_{i-\tau}$ and $x_{i-\delta}$ are aligned in time, i.e., $\delta = \tau$. This corresponds to the auto-correlation peak. As a result the correlation function can be rewritten as

$$\mathbf{R}_{h_0} = \mathbf{R}_h[\delta \neq \tau] = \sum_{i=1}^{L} (x_{i-\tau} x_{i-\delta}), \tag{4}$$

$$\mathbf{R}_{h_1} = \mathbf{R}_h[\delta = \tau] = \sum_{i=1}^{L} (x_{i-\tau} x_{i-\tau}), \tag{5}$$

where h_0 denotes events that the spreading codes are not aligned and h_1 denotes events in which the spreading codes are aligned. Although for each realization of the pilot sequence $x_{i-\tau}$ and $x_{i-\delta}$ are known, when all the possible chaotic pilot realizations are being examined, $x_{i-\tau}$ and $x_{i-\delta}$ will be random variables with the PDF given in (2). Now $\mathbf{R}_h[\delta]$ can be statistically modelled for both h_0 and h_1.

Considering (4), it is clear that $\mathbf{R}_{h_0}$ is the product of chaotic values summed for the correlation length for each trial. Given that for h trials both $x_{i-\tau}$ and $x_{i-\delta}$ are independent random variables, it is possible to find the distribution of the product of these and subsequently find the distribution of $\mathbf{R}_{h_0}$. However, noting that the correlation in tracking is performed over a large correlation period (typically $L > 100$), the correlation result will be the sum of many independent, identically distributed, random variables. As a result, central limit theorem can be invoked with a high degree of accuracy which gives the PDF of (4) as Gaussian.

In order to describe (4) statistically, the mean and variance are also needed. Therefore,

$$\begin{aligned} \mathrm{E}[\mathbf{R}_{h_0}] &= \mathrm{E}\left[\sum_{i=1}^{L} (x_{i-\tau} x_{i-\delta})\right] \\ &= L \times \mathrm{E}[x_{i-\tau}]\mathrm{E}[x_{i-\delta}] \\ &= 0, \end{aligned} \tag{6}$$

where $E[\cdot]$ denotes the expected value.

The variance can be determined as follows:

$$\begin{aligned} \sigma^2_{\mathbf{R}_{h_0}} &= \mathrm{E}\left[\mathbf{R}^2_{h_0}\right] - \mathrm{E}^2[\mathbf{R}_{h_0}] \\ &= \sum_{i=1}^{L} \mathrm{E}\left[x^2_{i-\tau}\right] \mathrm{E}\left[x^2_{i-\delta}\right] \\ &= \frac{L}{4}. \end{aligned} \tag{7}$$

In the above formula since $\mathrm{E}[x] = 0$, $\mathrm{E}[x^2] = \sigma_x^2$.

Given the above,

$$\mathbf{R}_{h_0} \sim G\left(0, \frac{L}{4}\right), \tag{8}$$

which is a Gaussian distribution that describes the statistical behavior of $\mathbf{R}_h[\delta \neq \tau]$.

Similarly considering (5), $\mathbf{R}_{h_1}$ can be modeled as a random variable with a Gaussian distribution with the mean and variance of

$$\begin{aligned}\mathrm{E}[\mathbf{R}_{h_1}] &= \mathrm{E}\left[\sum_{i=1}^{L}\left(x_{i-\tau}^2\right)\right] \\ &= \frac{L}{2},\end{aligned} \tag{9}$$

and

$$\begin{aligned}\sigma_{\mathbf{R}_{h_1}}^2 &= \mathrm{E}\left[\mathbf{R}_{h_1}^2\right] - \mathrm{E}^2[\mathbf{R}_{h_1}] \\ &= \sum_{i=1}^{L}\left\{\mathrm{E}\left[x_{i-\tau}^4\right] - \mathrm{E}^2\left[x_{i-\tau}^2\right]\right\} \\ &= L\left\{\frac{3}{8} - \frac{1}{4}\right\} \\ &= \frac{L}{8},\end{aligned} \tag{10}$$

respectively.

Therefore, $\mathbf{R}_{h_1}$ can be statistically expressed as

$$\mathbf{R}_{h_1} \sim G\left(\frac{L}{2}, \frac{L}{8}\right), \tag{11}$$

which is a Gaussian distribution that describes the statistical behavior of the auto-correlation peak of the chaotic spreading codes.

Considering the case where additive white Gaussian noise (AWGN), the two PDFs can be reexpressed as

$$\mathbf{R}_h[\delta] \sim \begin{cases} G\left(0, \frac{L}{4} + \frac{L\sigma_N^2}{2}\right) & \delta \neq \tau \\ G\left(\frac{L}{2}, \frac{L}{8} + \frac{L\sigma_N^2}{2}\right) & \delta = \tau, \end{cases} \tag{12}$$

where $\sigma_{\mathbf{N}}^2$ is the residual noise variance and it is assumed that $\mathrm{E}[\mathbf{N}] = 0$.

Since the tracking loop is noncoherent, each branch has a square-law device that squares every sample of $\mathbf{R}_h[\delta]$ given above. The PDF of the squared correlation function can be expressed for $\mathbf{R}_{h_0}$ and $\mathbf{R}_{h_1}$ separately.

If $\mathbf{R}_{h_0}$ is squared and then normalized by its variance, the result is a chi-square distribution with one degree of freedom with the PDF

$$P\left(\mathbf{R}'_{h_0}, 1\right) = \frac{1}{\sqrt{2\pi\mathbf{R}'_{h_0}}} \exp\left(\frac{-\mathbf{R}'_{h_0}}{2}\right), \tag{13}$$

where $\mathbf{R}'_{h_0} = \mathbf{R}_{h_0}^2/\sigma_{\mathbf{R}_{h_0}}^2$.

If $\mathbf{R}_{h_1}$ is squared and then normalized by its variance, the resulting distribution is noncentral chi-square with one degree of freedom and the noncentrality parameter λ. The PDF can then be expressed as (14) at the bottom of the page where $\mathbf{R}'_{h_1} = \mathbf{R}_{h_1}^2/\sigma_{\mathbf{R}_{h_1}}^2$, $\lambda = 2L/1 + 4\sigma_{\mathbf{N}}^2$, and $I(.)$ is the modified Bessel function of the first kind.

As can be seen form the derivation above, the correlation function of a chaotic spreading code is now expressed using a statistical model. Given that the correlation function of the chaotic codes changes with every trial, this statistical approach is much more useful in describing the behavior as opposed to the traditional method of expressing the correlation function used for binary type spreading codes. The analysis presented above is valid for long sequence lengths. It has been shown in [30] that the short sequence length does not follow a Gaussian distribution. However, normally the sequence length for tracking has to be long enough to allow sufficient resolution for *fine synchronization*.

IV. Applying the Statistical Model to the Chaos-Based Noncoherent Tracking Loop

In this section, the statistical chaotic correlation function model will be applied to the chaos-based noncoherent tracking loop. The statistical correlation function method is not limited to chaos-based systems, and it can be applied to all nonbinary spreading codes.

There are two issues to be considered here: first, the tracking loop filters cannot attenuate all the noise terms to zero and there always remains some residue noise which has to be taken into account in the statistical analysis of $D_\Delta(\delta)$. Therefore, from now on, the statistical analysis will focus on $D_\Delta(\delta)$ with the understanding that the correlation functions will have some residue noise in them. Second, although $D_\Delta(\delta)$ is ideally a dc term for conventional binary spreading codes, for chaotic spreading codes it is only so for one representation of the tracking loop. If many experiments are performed for the same chaotic map, $D_\Delta(\delta)$ will have a distribution even in the noiseless case because the correlation function of chaotic spreading codes varies with the change of the spreading code.

$$P\left(\mathbf{R}'_{h_1}; 1, \lambda\right) = \frac{1}{2}\exp\left(\frac{-\mathbf{R}'_{h_1} + \lambda}{2}\right)\left(\frac{\mathbf{R}'_{h_1}}{\lambda}\right)^{-1/4} I_{-1/2}\left(\sqrt{\mathbf{R}'_{h_1}\lambda}\right), \tag{14}$$

The statistical error signal will be denoted by $\mathbf{D}_{\Delta}(\delta)$. It has to be noted that $D_{\Delta}(\delta)$ which was explained in Section II is only one instance of $\mathbf{D}_{\Delta}(\delta)$. The statistical input to the voltage controlled oscillator, $\mathbf{D}_{\Delta}(\delta)$, is expressed as

$$\mathbf{D}_{\Delta}(\delta) = \mathbf{R}^2\left[\left(\delta - \frac{\Delta}{2}\right)T_c\right] - \mathbf{R}^2\left[\left(\delta + \frac{\Delta}{2}\right)T_c\right]. \quad (15)$$

The above expression is the difference of two statistical correlation functions that are squared. Noting the discussion in Section III, the square of each correlation function follows the distributions given in (13) and (14) depending on the spreading code alignment. That is, the peaks of the correlation function follow the noncentral chi-square distribution given in (14) and the other values in the correlation function, follow the central chi-square distribution given in (13).

It has to be noted that the two functions have a relative time delay. This is a crucial fact in determining the distribution of the various points of the tracking loop S-curve. It is assumed that the time separation between the advanced and delayed correlators equals one chip duration, i.e., $\Delta = 1$. This is the most common value used in literature [10] and the analysis is similar for all Δ as long as $0 < \Delta \leqslant 1$.

It is observed from (15) that when in the one correlator $\delta = \tau$, in the other $\delta \neq \tau$. In other words, when one correlator is at its peak, the other one has a small value. This is illustrated in Fig. 3 which shows the output of the two square-law devices with a time difference of one chip duration, that is $\Delta = 1$.

To statistically model $\mathbf{D}_{\Delta}(\delta)$, it is sufficient to find the distribution of two points on the S-curve. Fig. 4 shows these points as A and B. Point A represents the instance that $\delta = 0.5$ and point B represents $\delta = 0$ instance. Fig. 4 also presents the chosen statistical bounds of 0.1 and 4 standard deviations as well as the common assumption about the S-curve presented in [16]–[18]. It is now clear that the value at the positive peak (point A) can be found by subtracting $\mathbf{R}'_{h_0}$ from $\mathbf{R}'_{h_1}$, which means that the distribution at this point can be found by convolving the distributions of $\mathbf{R}'_{h_0}$ and $\mathbf{R}'_{h_1}$ which are given in (13) and (14) respectively. This is shown in the form of a convolution integral in (16) at the bottom of the page where $*$ denotes convolution. The negative peak can be analyzed in exactly the same way with a change of sign. The solution of the convolution integral given in (16) is not tractable; therefore, a numerical solution is performed with the result given in Section V.

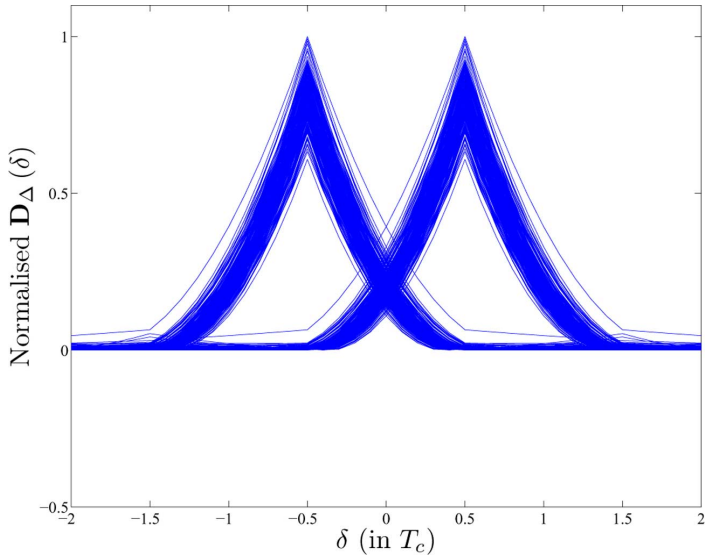

Fig. 3. The outputs of the square-law devices for the two branches of the tracking loop. When one correlation is at its peak the other one has a small value.

Similarly, the value at point B in Fig. 4 is the subtraction of $\mathbf{R}'_{h_0}$ in one correlation function from the other. The distribution at point B can be found by convolving two distributions of $\mathbf{R}'_{h_0}$ given in (13). It has to be noted that since the convolution of two central chi-square distributions is another chi-square distribution with the summation of degrees of freedom, then the distribution of the centre part of $\mathbf{D}_{\Delta}(\delta)$ can be expressed as (17) without the need to do the actual integration.

It is important to compare the correlation properties of the chaos-based sequences with the conventional binary ones. This comparison can be done by mathematically describing the correlation function and the S-curve for binary sequences and comparing them to what was presented in Section IV. In this paper, the maximal length sequences (m-sequences) has been chosen for the comparison.

The first point to consider is that the correlation function of m-sequences is only dependant on the correlation length and will remain fixed if another m-sequence is used. This is unlike the chaotic sequences which have slightly different correlation

$$P\left(\mathbf{R}'_{h_1};1,\lambda\right) * P\left(\mathbf{R}'_{h_0},1\right) = \frac{1}{2}\int_{-\infty}^{\infty} \frac{1}{\sqrt{2\pi(\mathbf{R}'_h - \tau)}} \exp\left(\frac{-(\mathbf{R}'_h - \tau)}{2}\right) \times \left\{\exp\left(\frac{-(\tau+\lambda)}{2}\right) + \left(\frac{\tau}{\lambda}\right)^{-1/4} + I_{-1/2}\sqrt{\tau\lambda}\right\} d\tau \quad (16)$$

$$P\left(\mathbf{R}'_{h_0},1\right) * P\left(\mathbf{R}'_{h_0},1\right) = P\left(\mathbf{R}'_{h_0},2\right) = \frac{1}{2}\exp\left(\frac{-(\mathbf{R}'_{h_0})}{2}\right)$$

$$\lim_{\mathbf{R}'_{h_0}\to+\infty} P\left(\mathbf{R}'_{h_0},1\right) * P\left(\mathbf{R}'_{h_0},1\right) = 0 \quad (17)$$

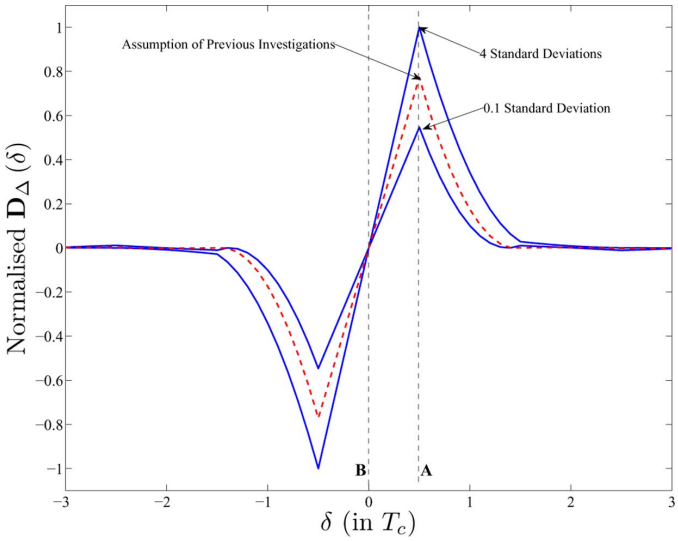

Fig. 4. Upper and lower limits of the S-curve as well as the chosen points for the distribution. The assumption used [16], [17] is shown with a dashed line.

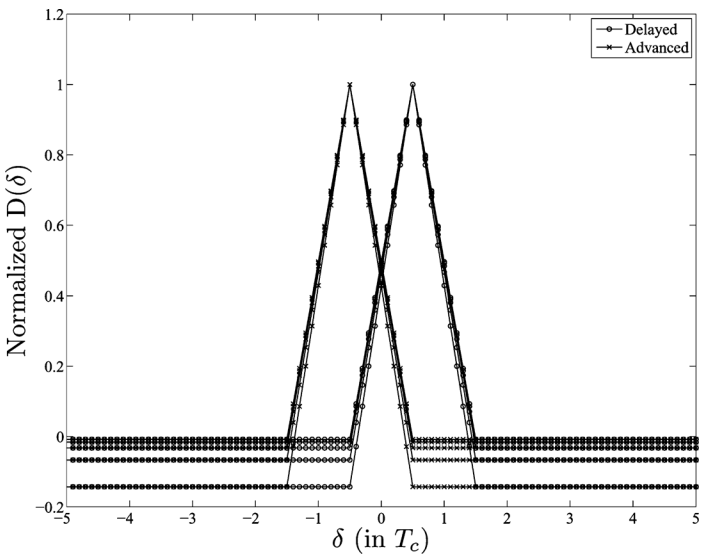

Fig. 5. Early and late correlation functions for correlation lengths of 8, 16, 32, 64, and 128 before the square law device.

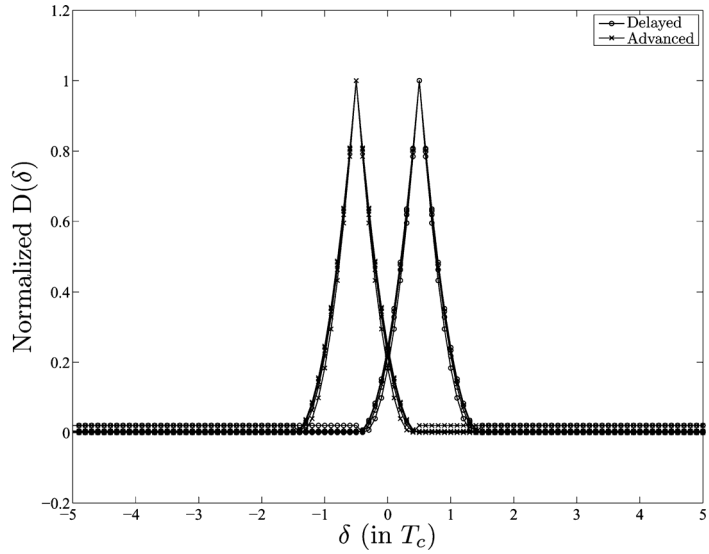

Fig. 6. Early and late correlation functions for correlation lengths of 8, 16, 32, 64, and 128 after the square law device.

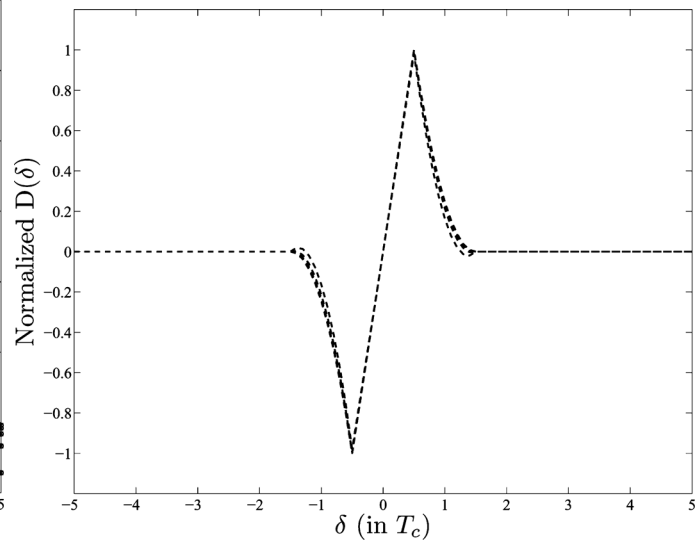

Fig. 7. $D_{\Delta_b}(\delta)$ for correlation lengths of 8, 16, 32, 64, and 128.

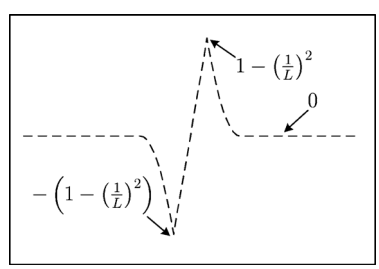

Fig. 8. Theoretical values for $D_{\Delta_b}(\delta)$ in a noncoherent scenario.

function values for different sequences. The early and late correlation functions for m-sequences are presented in Fig. 5. It should be noted that these correlation functions are before the square law-device. As can be seen in Fig. 5 different correlation lengths affect the dc offset of the correlation functions; however, the peak of the correlation functions remain at 1 no matter what the correlation length is.

In noncoherent tracking, square law devices have to be used and the early-late correlation functions presented in Fig. 5 will change to the ones presented in Fig. 6. Two matters are of interest in Fig. 6, the first is the nonlinearity which is introduced to the correlation functions, and the second is the change in the dc offset for the correlation functions; both of these are expected because of the squaring.

To clearly distinguish the S-curves of binary from the chaotic sequences, $D_{\Delta_b}(\delta)$ is used as the notation referring to the binary S-curve. Using this notation, it can be seen in Fig. 7 that the only factor that changes the $D_{\Delta_b}(\delta)$ is the correlation length which has been changed in the range of 8–128 chips. The main difference between the $D_{\Delta_b}(\delta)$ presented in Fig. 7 and $\mathbf{D}_\Delta(\delta)$ presented in Fig. 4 is the fact that the chaotic S-curve has to be described with a statistical distribution, whereas the $D_{\Delta_b}(\delta)$ is a fixed entity. Finally, Fig. 8 shows the theoretical values for $D_{\Delta_b}(\delta)$ in the noncoherent scenario.

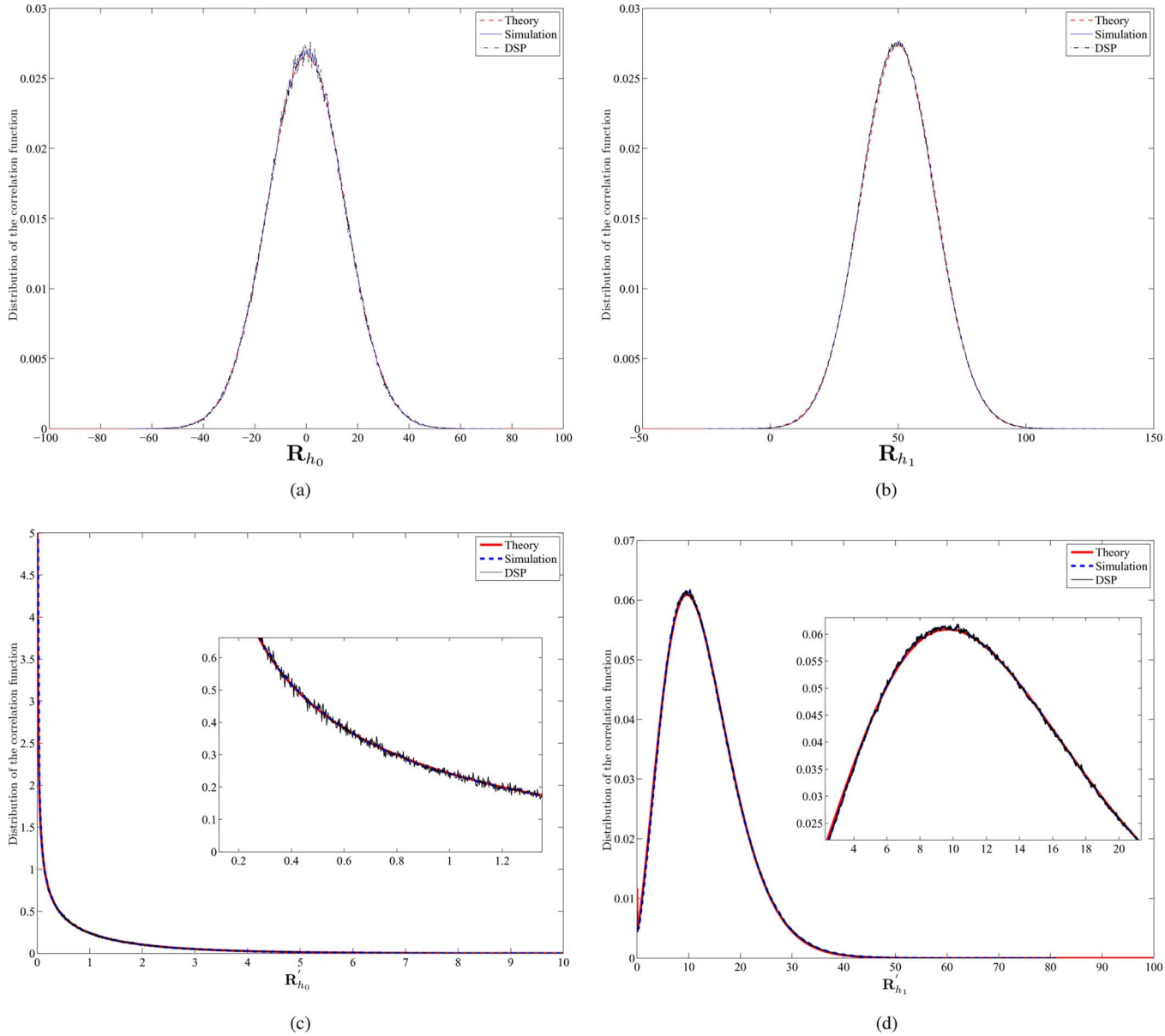

Fig. 9. Comparison between the statistical model predictions of the correlation function of chaotic spreading codes with the simulation results. (a) Theoretical and simulation results for $\mathbf{R}_{h_0}$. (b) Theoretical and simulation results for $\mathbf{R}_{h_1}$. (c) Theoretical and simulation results for $\mathbf{R}'_{h_0}$. (d) Theoretical and simulation results for $\mathbf{R}'_{h_1}$.

V. Comparison of the Theoretical Model With Simulation and Hardware Implementation

In order to verify the theoretical findings, simulations were performed for each stage of the statistical analysis. The results of these simulations were then compared to the theoretical results derived in Section IV as well as hardware implementation results. For hardware implementation a digital signal processor (DSP) was used. The DSP chosen for this investigation is the ADSP-TS201 S TigerSHARC from Analog Devices which is designed with signal processing and large scale telecommunication tasks in mind. This DSP supports single-precision IEEE 32-bit and extended-precision 40-bit floating-point data formats as well as 8-, 16-, 32-, and 64-bit fixed-point data formats. Based on the tests performed, a word length of 32 was chosen as it contained sufficient precision for the generation of the chaotic samples. The DSP also has a sufficiently wide dynamic range to allow the implementation of an AWGN generator and has a processor clock speed of 600 MHz and is capable of executing 2400 MIPS, 3600 MFLOPS, and 1200 MMACS. Overall, the capabilities of this DSP were deemed sufficient for the purposes of prototyping the chaos-based noncoherent tracking loop presented [31].

As can be seen from Fig. 9, the statistical method proposed in this paper has a very high accuracy for predicting the distributions of the chaotic correlation function. The mean and variances predicted are followed closely by the simulation for both $\mathbf{R}_{h_0}$ and $\mathbf{R}_{h_1}$. Also, the chi-square distributions closely match the squared values which are taken from the tracking loop.

The first set of results are presented to show the accuracy of the CCS method used. To simulate this, a statistically significant number of chaotic-correlation functions were formed from the

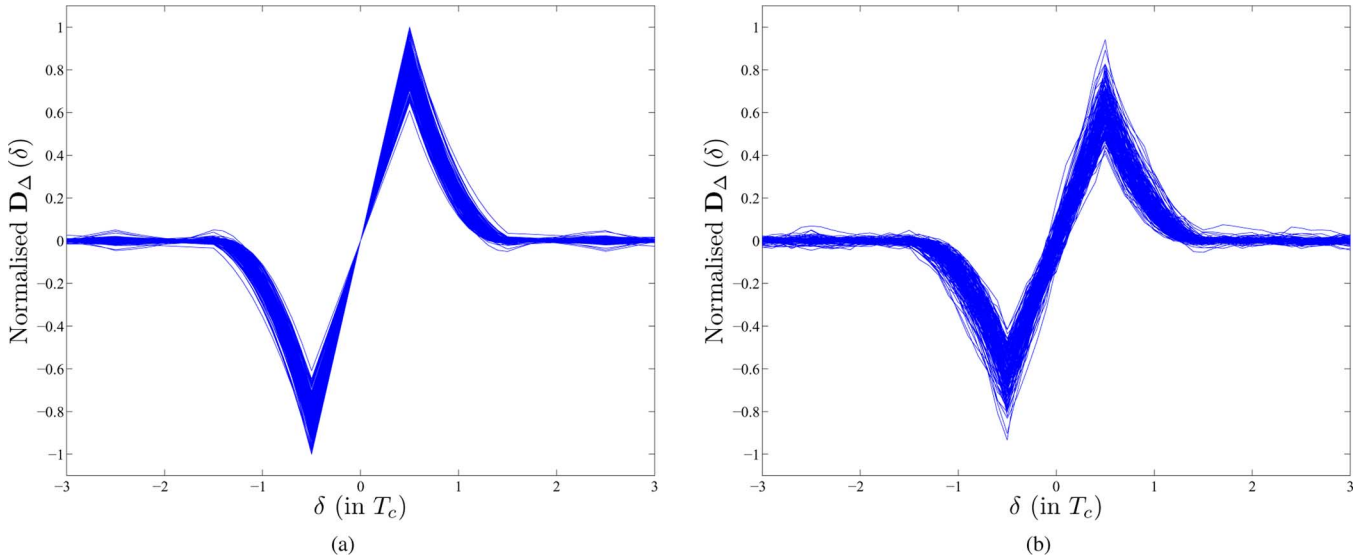

Fig. 10. $\mathbf{D}_\Delta(\delta)$ in the chaos-based noncoherent tracking loop, noiseless (a) and SNR $= -12$ dB (b).

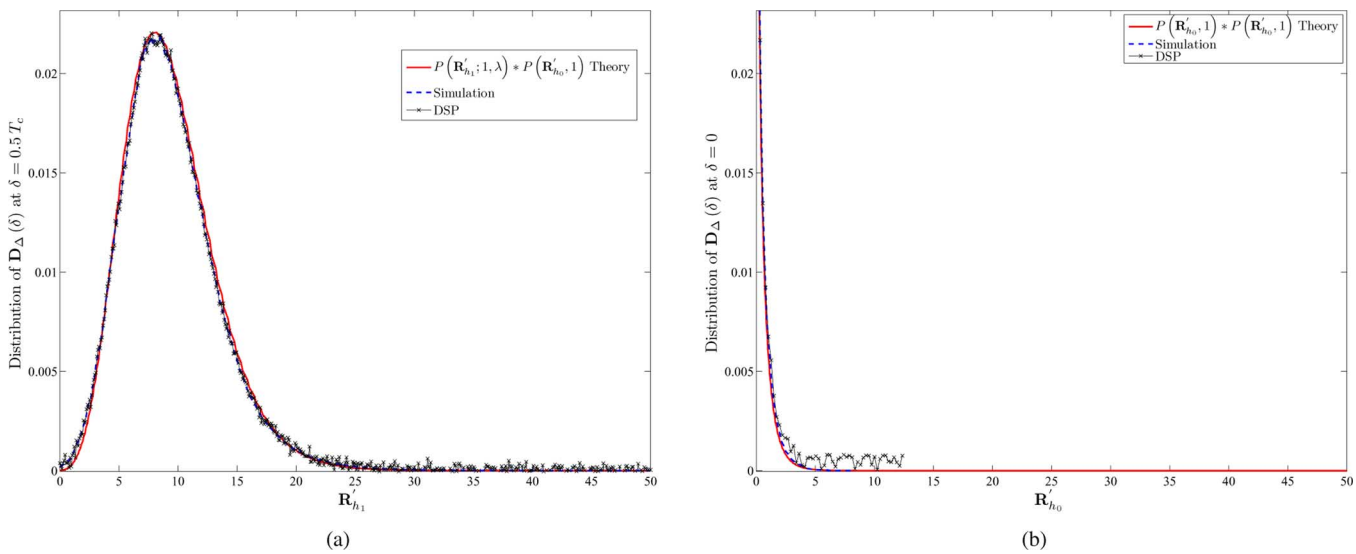

Fig. 11. The distribution of $\mathbf{D}_\Delta(\delta)$ for $\delta = 0, 0.5T_c$.

logistic map using different initial conditions. The cross-correlation and auto-correlation peaks of these functions were then recorded and their distributions were drawn with the correlation length chosen to be 100 ($L = 100$). The distribution of $\mathbf{R}_{h_0}$ is shown in Fig. 9(a) and is a zero mean Gaussian distribution. The theoretical prediction is followed closely by the DSP and simulation results. Fig. 9(b) shows the distribution for $\mathbf{R}_{h_1}$ with the mean in this case being $L/2 = 50$. The two distributions will go through the square-law device. Fig. 9(c) and (d) show the distributions for $\mathbf{R}'_{h_0}$ and $\mathbf{R}'_{h_1}$ respectively. In order to show the accuracy of the proposed method, insets are provided within these figures showing a more detailed rendition of the area of interest.

The simulation setup for the chaos-based noncoherent tracking loop involved generating a statistically significant number of S-curves and observing their distributions at the points shown in Fig. 3. Fig. 10(a) shows the noiseless $\mathbf{D}_\Delta(\delta)$ values for $\Delta = 1$. It can be observed that, even in the noiseless case, the peaks of $\mathbf{D}_\Delta(\delta)$ have a distribution. It also should be noted that the slope in the linear region of the noiseless graph, changes because of the distribution of the peaks, unlike the previous assumptions in literature. The effect of noise in Fig. 10(b) is shown as the horizontal movement of the S-curves. It has to be noted that noise changes the place of the zero crossing on the $\mathbf{D}_\Delta(\delta)$ curve. Also, the SNR of -12 dB is calculated using the chip energy value that is, $E_c/N_0 = -12$ dB.

Another point relates to the multiple access SS (MA-SS) systems and their relationship with the current analysis here. It has to be noted that the addition of other users' spreading codes to the pilot which is being tracked only adds to the validity of the Gaussian analysis presented here. The only statistical effect which adding multiple users will cause is an increase in the variance of the correlation function which is a manifestation of interuser-interference and is detrimental to the system performance.

Fig. 11(a) shows the comparison between the theoretical results obtained by evaluating the integral given in (16) numerically and the simulation and DSP results which have been ob-

tained by subtracting the values of the two correlators over a large experiment space. Similarly Fig. 11(b) shows the same comparison but for the integral given in (17). As can be seen the results match closely, the slight differences are due to the numerical evaluation of the integral as well as the resolution of the DSP.

VI. Conclusions

In this paper, a chaos-based noncoherent tracking loop is analyzed using CCS. The governing equation is then derived using the CCS approach and then compared to the simulation and hardware implementation results with close agreement. It is shown that the conventional treatment of binary spreading codes is not suitable to analyze nonbinary codes including chaotic spreading codes because it assumes the correlation function of the chaotic sequences to be constant. The proposed CCS method addresses this issue and gives the ability of properly describing the behavior and performance of the chaos-based noncoherent tracking loop.

Acknowledgment

The authors wish to thank Prof. G. Setti and the anonymous reviewers for their useful comments.

References

[1] C. E. Shannon, "Communication theory of secrecy systems," *Bell Syst. Tech. J.*, vol. 28, pp. 656–715, 1949.

[2] P. Stavroulakis, *Chaos Applications in Telecommunications*. Boca Raton, FL: CRC, 2006.

[3] W. Tam, F. Lau, C. Tse, and A. Lawrance, "Exact analytical bit error rates for multiple access chaos-based communication systems," *IEEE Trans. Circuits Syst. II, Exp. Briefs*, vol. 51, no. 9, pp. 473–481, Sep. 2004.

[4] M. P. Kennedy, R. Rovatti, and G. Setti, *Chaotic Electronics in Telecommunications*. Boca Raton, FL: CRC, 2000.

[5] F. Lau and C. Tse, *Chaos-Based Digital Communicaion Systems*. Berlin, Germany: Springer, 2004.

[6] W. M. Tam, F. C. M. Lau, and C. K. Tse, "A multiple access scheme for chaos-based digital communication systems utilizing transmitted reference," *IEEE Trans. Circuits Syst. I, Reg. Papers*, vol. 51, no. 9, pp. 1868–1878, Sep. 2004.

[7] R. Rovatti, G. Mazzini, and G. Setti, "On the ultimate limits of chaos-based asynchronous DS-CDMA-II: Analytical results and asymptotics," *IEEE Trans. Circuits Syst. I, Reg. Papers*, vol. 51, no. 7, pp. 1348–1364, Jul. 2004.

[8] G. Setti, R. Rovatti, and G. Mazzini, "Performance of chaos-based asynchronous DS-CDMA with different pulse shapes," *IEEE Commun. Lett.*, vol. 8, no. 7, pp. 416–418, Jul. 2004.

[9] G. Kaddoum, D. Roviras, P. Charge, and D. Fournier-Prunaret, "Robust synchronization for asynchronous multi-user chaos-based DS-CDMA," *Signal Process.*, vol. 89, no. 5, pp. 807–818, 2009.

[10] R. L. Peterson, R. E. Zeimer, and D. E. Borth, *Introduction to Spread Spectrum Communicaion*. Englewood Cliffs, NJ: Prentice-Hall, 1995.

[11] M. K. Simon, J. K. Omura, R. A. Scholtz, and B. K. Levitt, *Spread Spectrum Handbook*. New York: McGraw-Hill, Inc., 2002.

[12] L. Hanzo, L. Yang, E. Kuan, and K. Yen, *Single and Multi-Carrier DS-CDMA Multi-User Detection, Space-Time Spreading, Synchronisation and Starndards*. Chichester, U.K.: IEEE Press Wiley, 2003.

[13] J. J. Spilker and D. Magill, "The delay-lock discriminator-an optimum tracking device," *Proc. IRE*, vol. 9, pp. 1403–1416, 1961.

[14] J. J. Spilker, *Digital Communications by Satellite*, ser. Prentice-Hall information and system sciences. Englewood Cliffs, N.J.: Prentice-Hall, 1977.

[15] G. Setti, R. Rovatti, and G. Mazzini, "Synchronization mechanism and optimization of spreading sequences in chaos-based DS-CDMA systems," *IEICE Trans. Fundam. Electron., Commun., Comput. Sci.*, vol. E82-A, no. 9, pp. 1737–1746, Sep. 1999.

[16] R. Vali, S. Berber, and S. K. Nguang, "Analysis of a chaos-based non-coherent delay lock tracking loop," in *Proc. IEEE Int. Conf. Commun. (ICC)*, May 2010, pp. 1–6.

[17] R. Vali, S. Berber, and S. Nguang, "Effect of Rayleigh fading on non-coherent sequence synchronization for multi-user chaos based DS-CDMA," *Signal Process.*, vol. 90, no. 6, pp. 1924–1939, 2010.

[18] R. Vali, S. Berber, and S. K. Nguang, *Planning and Optimisation of 3 G and 4 G Wireless Networks*. Aalborg, Denmark: River Publ., 2009, ch. Synchronization, pp. 445–479.

[19] A. Loria and A. Zavala-Rio, "Adaptive tracking control of chaotic systems with applications to synchronization," *IEEE Trans. Circuits Syst. I, Reg. Papers*, vol. 54, no. 9, pp. 2019–2029, Sep. 2007.

[20] J. C. Feng and C. Tse, "Identification and tracking of chaotic signals with application to non-coherent detection for chaos-based communications," in *Proc. Int. Conf. Commun., Circuits, Syst. (ICCCAS)*, Jun. 2004, vol. 2, pp. 851–854.

[21] J.-C. Feng, C. Tse, and F. Lau, "A chaos tracker applied to non-coherent detection in chaos-based digital communication systems," in *Proc. IEEE Int. Symp. Circuits Syst. (ISCAS)*, May 2001, vol. 3, pp. 795–798.

[22] T. Kohda, "Information sources using chaotic dynamics," *Proc. IEEE*, vol. 90, no. 5, pp. 641–661, May 2002.

[23] G. Setti, G. Mazzini, R. Rovatti, and S. Callegari, "Statistical modeling of discrete-time chaotic processes-basic finite-dimensional tools and applications," *Proc. IEEE*, vol. 90, no. 5, pp. 662–690, May 2002.

[24] T. A. Khan, N. Eshima, Y. Jitsumatsu, and T. Kohda, "Map code acquisition shows superiority of Bologna codes in a class of multiuser CDMA systems," in *Proc. Int. Symp. Nonlinear Theory Its Appl. (NOLTA 2005)* , Bruges, Belgium, pp. 94–97.

[25] T. A. Khan, N. Eshima, Y. Jitsumatsu, and T. Kohda, "Code acquisition in asynchronous DS/CDMA systems, Markov and i.i.d. codes in multiuser scenario," Proc. Int. Symp. Nonlinear Theory Its Appl. (NOLTA 2004). Fukuoka, Japan, pp. 689–692.

[26] T. Kohda and Y. Jitsumatsu, "Tradeoff between bit error rate and acquisition rate in an asynchronous DS/CDMA system," in *Proc. IEEE Int. Symp. Nonlinear Theory Its Appl.*, 2002.

[27] G. Cimatti, R. Rovatti, and G. Setti, "Chaos-based spreading in DS-UWB sensor networks increases available bit rate," *IEEE Trans. Circuits Syst. I, Reg. Papers*, vol. 54, no. 6, pp. 1327–1339, Jun. 2007.

[28] T. Geisel and V. Fairen, "Statistical properties of chaos in Chebyshev maps," *Phys. Lett.*, vol. 105A, pp. 263–266, 1984.

[29] S. Berber and B. Jovic, "Sequence synchronization in a wideband CDMA system," in *Proc. 2006 Int. Conf. Wirel. Broadband Ultra Wideband Commun. (AusWireless)*, Sydney, Australia, Mar. 13–16, 2006, pp. 1–6.

[30] G. Kaddoum, P. Chargé, D. Roviras, and D. Fournier-Prunaret, "A methodology for bit error rate prediction in chaos-based communication systems," *Circuits, Syst., Signal Process.*, vol. 28, pp. 925–944, 2009.

[31] Adsp-ts201 s: 500/600 mhz Tigersharc Processor Data Sheet Analogue Devices Inc, 2006, Tech. Rep.

Ramin Vali received the B.E. degree (honors) from the Department of Electrical and Computer Engineering, University of Auckland, New Zealand, in 2007. Currently, he working toward the Ph.D. degree in the same department.

He has published a number of peer reviewed conference and journal papers in the field of chaos-based spread spectrum communication systems. He has also been a reviewer for the IEEE Transactions on Wireless Communications. His research interests include: spread spectrum security, chaos-based communication systems and their synchronization, chaos-based CDMA, LTE, and OFDM communication systems.

Stevan M. Berber (M'00–SM'03) was born in Stanisic, Serbia, former Yugoslavia. He completed his undergraduate studies in electrical engineering in Zagreb, M.S. studies in Belgrade, and Ph.D. studies in Auckland, New Zealand.

Currently he is with the Department of Electrical and Computer Engineering at Auckland University, New Zealand. He was appointed Visiting Professor at the University of Novi Sad in 2004 and Visiting Scholar at the University of Sydney in 2008. His teaching interests are in communication systems, information and coding theory, discrete stochastic signal processing, and wireless sensor and computer networks. He is the author of more than 80 refereed journal and conference papers, 8 books and 3 book chapters. His research interests are in the fields of digital communication systems and signal processing with the emphasis on applications in CDMA systems and wireless computer, communication and sensor networks.

Dr. Berber is a referee for papers in leading journals and conferences in his research area. He has been leading or working on a large number of research and industry projects. He is a member of New Zealand Scientists and an accredited NAATI translator for English language.

Sing Kiong Nguang received the B.E. (with first class honours) and Ph.D. degrees from the Department of Electrical and Computer Engineering of the University of Newcastle, Australia, in 1992 and 1995, respectively.

Currently, he is with the Department of Electrical and Computer Engineering, University of Auckland, Auckland, New Zealand. He has published over 200 refereed journal and conference papers on nonlinear control design, nonlinear control systems, nonlinear time-delay systems, nonlinear sampled-data systems, biomedical systems modelling, fuzzy modelling and control, biological systems modelling and control, and food and bioproduct processing. He has/had served on the editorial board of a number of international journals. He is the Chief Editor of the *International Journal of Sensors, Wireless Communications and Control*.